Acta Cryst. (1981). B37, 2139–2142

$P_4W_8O_{32}$: A Mixed-Valence Tunnel Structure Built up of ReO_3-Type Slabs Connected through PO_4 Tetrahedra

By J. P. Giroult, M. Goreaud, Ph. Labbé and B. Raveau

Laboratoire de Cristallographie et Chimie du Solide, LA 251, *Institut des Sciences de la Matière et du Rayonnement, Université de Caen,* 14032 *Caen CEDEX, France*

(*Received* 16 *February* 1981; *accepted* 5 *May* 1981)

Abstract

The crystal structure of $P_4W_8O_{32}$ has been solved by three-dimensional single-crystal X-ray analysis. The refinements have been made in the space group $P2_12_12_1$ with $a = 5{\cdot}285$ (2), $b = 6{\cdot}569$ (1), $c = 17{\cdot}351$ (3) Å, leading to $R = 0{\cdot}058$ and $R_w = 0{\cdot}071$ for 967 independent reflections. The framework of this structure, built up of WO_6 octahedra and PO_4 tetrahedra, can be described as ReO_3-type slabs connected through PO_4 tetrahedra. This type of connection creates pentagonal tunnels in the [100] direction. Two sorts of empty cages are formed, limited by twelve or eighteen O atoms. The possibility of insertion of cations in the cavities of the structure and the existence of microphases $P_4W_{4n}O_{12n+8}$ are discussed.

Introduction

The capability of the pyrophosphate group to accommodate an octahedral framework is now well established in the case of ternary tungsten oxides. Investigating the P_2O_5–WO_3 system, Schulz (1955) has indeed isolated the oxides $P_2O_5.WO_3$ and $P_2O_5.2WO_3$ and Kierkegaard (1958) has published a structural study of the first one, which is built up of WO_6 octahedra and P_2O_7 groups sharing their corners. Our recent studies (Giroult, Goreaud, Labbé & Raveau, 1980, 1981) have allowed us to synthesize a series of microphases $Rb_xP_8W_{8n}O_{24n+16}$, whose host lattice is built up of ReO_3-type slabs interconnected through P_2O_7 groups, forming distorted hexagonal tunnels where the Rb^+ ions are located. Moreover, in the latter structures, the mixed valence of tungsten raises the possibility that these phases may be metallic. It thus seemed exciting to investigate the more simple W—P—O system, where W is able to take an oxidation state less than six.

The present work deals with the structure of $P_4W_8O_{32}$ in which tungsten has an apparent oxidation state of 5·5.

Experimental

Sample preparation

Mixtures of $(NH_4)_2HPO_4$ and WO_3 in appropriate ratios were first heated in air at 1173 K to decompose the phosphate; the resultant products were then mixed with adequate amounts of metallic tungsten and heated for four days at 1250 K in evacuated silica ampoules. Powder patterns of the samples showed a pure phase for the composition PW_2O_8 and have been indexed in the orthorhombic cell, deduced from a preliminary single-crystal study, with the refined parameters $a = 5{\cdot}28$ (2), $b = 6{\cdot}57$ (2), $c = 17{\cdot}37$ (5) Å.

Structure determination

The crystals were generally red plates. Films obtained with a Weissenberg camera show orthorhombic symmetry. The measured cell parameters were confirmed later by diffractometric techniques with a least-squares refinement based on 25 reflections of the reciprocal space: $a = 5{\cdot}285$ (2), $b = 6{\cdot}569$ (1) and $c = 17{\cdot}351$ (3) Å. The only systematic absences: $h00$, $h = 2n + 1$; $0k0$, $k = 2n + 1$ and $00l$, $l = 2n + 1$, led to the space group $P2_12_12_1$.

The crystal selected for the data collection was a plate parallel to (001) with a hexagonal section limited by {110} and {010}, and dimensions 192 × 72 × 36 µm. The data were collected with a CAD-4 Enraf–Nonius diffractometer with Mo $K\alpha$ radiation filtered with a graphite monochromator. The intensities were measured up to $2\theta = 90°$ with the ω–2θ technique with a maximum scan width of 1·40° and a counter slit aperture extended to 3°. The background intensity was measured on both sides of each reflection. A periodic control verified the stability of the sample. Among 2423 measurements with $\sigma(I)/I < 0{\cdot}70$ in two equivalent spaces, only 967 independent reflections were common to both spaces and considered to have a significant value. These were corrected for Lorentz and polarization effects. Absorption corrections were made

0567-7408/81/122139-04\$01.00

with a program based on the crystal morphology. The minimum and maximum transmission factors were 0·078 and 0·280. Nevertheless, during the refinement this last correction led curiously to non-significant values for atomic thermal coefficients, and afterwards this absorption correction was omitted.

The structure was solved by the heavy-atom method. All the tungsten atom positions were fixed by a Patterson function and refined by least-squares techniques. All P and O atoms were then located during subsequent difference syntheses. Scattering factors for W and P atoms were from Cromer & Waber (1965), corrected for anomalous dispersion (Cromer, 1965), and for O^{2-} from Suzuki (1960). A linear weighting scheme was adjusted according to $\langle w|F_o| - |F_c|\rangle$ in terms of sin θ/λ. The refinement with anisotropic thermal coefficients for W and isotropic for P and O atoms led to $R = \sum||F_o| - |F_c||/\sum|F_o| = 0{\cdot}058$ and $R_w = [\sum w(|F_o| - |F_c|)^2/\sum w|F_o|^2]^{1/2} = 0{\cdot}071$.* Final atomic parameters are given in Table 1. A projection of atomic positions onto (100) is shown in Fig. 1. The enantiomorphic structure, obtained by exchange of all atom coordinates xyz into $\bar{x}\bar{y}\bar{z}$, was also tested with and without absorption corrections, but gave less satisfactory results.

Table 1. *Positional parameters with e.s.d.'s for* $P_4W_8O_{32}$

$$B_{\text{eq}} = \tfrac{4}{3}\textstyle\sum_i\sum_j \beta_{ij}\,\mathbf{a}_i.\,\mathbf{a}_j.$$

	x	y	z	B (Å^2)
W(1)	0·2425 (11)	0·4119 (2)	0·04479 (8)	$B_{\text{eq}} = 0{\cdot}32$ (2)
W(2)	0·2560 (9)	0·2478 (2)	0·37239 (7)	$B_{\text{eq}} = 0{\cdot}25$ (2)
P	0·235 (3)	0·0524 (11)	0·1870 (4)	0·21 (10)
O(1)	−0·033 (7)	0·262 (7)	0·007 (2)	1·0 (5)
O(2)	0·243 (15)	0·245 (5)	0·1395 (15)	1·0 (3)
O(3)	0·261 (12)	0·117 (4)	0·2710 (14)	0·7 (3)
O(4)	−0·015 (6)	0·102 (5)	0·4037 (19)	0·3 (4)
O(5)	0·492 (6)	0·062 (5)	0·4111 (19)	0·4 (4)
O(6)	0·553 (6)	0·414 (5)	0·3332 (15)	0·3 (3)
O(7)	0·014 (7)	0·444 (5)	0·319 (2)	0·8 (4)
O(8)	0·251 (9)	0·408 (5)	0·4658 (17)	1·3 (5)

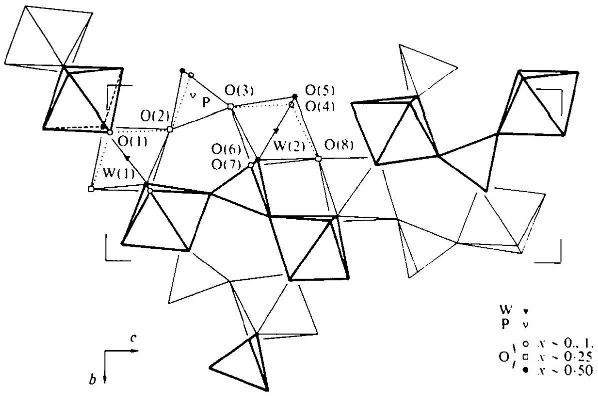

Fig. 1. Projection of the structure onto (100).

Description of the structure and discussion

The structure of this compound is built up of corner-sharing PO_4 tetrahedra and WO_6 octahedra (Fig. 1) and can be described by the coupling of zigzag chains parallel to the c axis and running at levels $x \simeq \frac{1}{4}$ and $\frac{3}{4}$. These chains, formed by units of two WO_6 octahedra and one PO_4 tetrahedron, are linked together through their oxygen atoms lying at $x \simeq 0$ and $\frac{1}{2}$ (Fig. 6*b*). This framework differs from the previous oxides (Giroult *et al.*, 1980, 1981) where it was necessary for the P_2O_7 groups to accommodate an octahedral framework. Here, the PO_4 tetrahedra are isolated since each PO_4 tetrahedron shares its corners with four WO_6 octahedra whose centres are located at the apices of an almost regular tetrahedron (Fig. 2). The two symmetrically independent tungsten atoms, W(1) and W(2), must be distinguished: the $W(1)O_6$ octahedra share their corners with one tetrahedron and five other octahedra in such a way that W(1) is octahedrally surrounded by 2W(1) + 3W(2) + 1P (Fig. 3*a*); the $W(2)O_6$ octahedra are linked to three octahedra and three tetrahedra whose centres also form an octahedron [3W(1) + 3P] but it is more distorted (Fig. 3*b*), although, in both cases, W(1) and W(2) are lying at a short distance (0·13 Å) from the centre of gravity of their surrounding W and P neighbours.

The geometry of the PO_4 and WO_6 polyhedra has been studied and the distances and angles are given in Table 2. Comparison of the PO_4 tetrahedron with those of the P_2O_7 groups in $Rb_xP_8W_{32}P_{112}$ (Giroult *et al.*, 1980) and in $Rb_xP_8W_{24}O_{88}$ (Giroult *et al.*, 1981) shows a large difference in that the isolated PO_4 tetrahedron in $P_4W_8O_{32}$ is quite regular, whereas in P_2O_7 groups one observes a distortion due to a

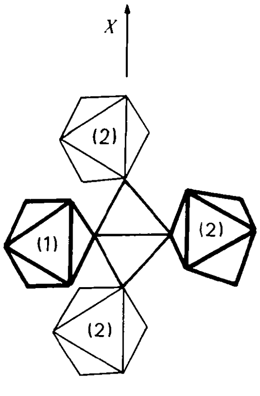

Fig. 2. Scheme of the tetrahedral surrounding of PO_4, viewed in the **b** direction. $W(1)O_6$ and $W(2)O_6$ octahedra are labelled (1) and (2).

---

* Lists of structure factors and anisotropic thermal parameters have been deposited with the British Library Lending Division as Supplementary Publication No. SUP 36179 (8 pp.). Copies may be obtained through The Executive Secretary, International Union of Crystallography 5 Abbey Square, Chester CH1 2HU, England.

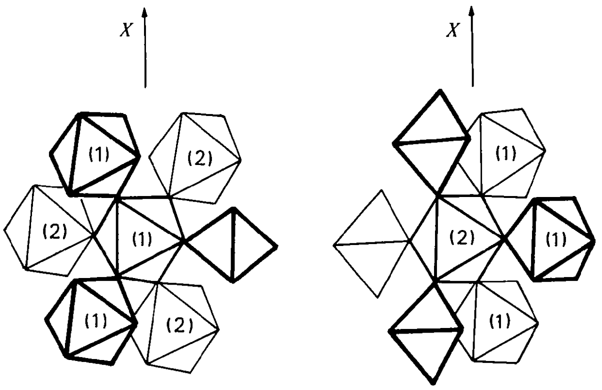

(a) (b)

Fig. 3. Scheme of the octahedral surrounding (a) for a $W(1)O_6$ octahedron, (b) for a $W(2)O_6$ octahedron, viewed in the **b** direction. $W(1)O_6$ and $W(2)O_6$ octahedra are labelled (1) and (2).

repulsion among the P atoms. Concerning the W atoms, it is interesting to compare their coordination in the present structure to that of W in the family $Rb_xP_8W_{8n}O_{24n+16}$, and the hexagonal bronzes In_xWO_3 (Labbé, Goreaud, Raveau & Monier, 1979) and other structures (Magnéli, 1956). In the present structure, the coordination of the W(1) atom is almost regular and its displacement from the centre of gravity of O atoms is only 0·07 (3) Å. For W(2), the coordination is rather 4 + 2 and the displacement 0·11 (3) Å. If we consider the different situations of the W atoms in the structures we have previously studied and in $P_4W_8O_{32}$, it appears that the distortion of a WO_6 octahedron increases with the mean oxidation state of W and with the number of covalent bonds P—O which are opposite the W—O bonds. When there are no W—O—P bonds, it seems that a WO_6 octahedron is quite regular if the mean oxidation state is less than about 5·66, the value we found in In_xWO_3. It is equally the case in $Rb_{1.82}P_8W_{24}O_{88}$ (oxidation state 5·59) for $W(2)O_6$ which is only linked with other octahedra. In the present compound, the oxidation state is 5·5 and that explains why $W(1)O_6$, which is linked with only one PO_4, is almost regular, whereas $W(2)O_6$ is distorted with the three longest W—O bonds corresponding to the three PO_4 neighbours.

The projection onto (100) shows that the framework delimits pentagonal tunnels running along the *a* axis (Fig. 1). These tunnels result from the stacking along **a** of pentagonal rings made of two PO_4 tetrahedra and three WO_6 octahedra. The pentagonal tunnels are narrower than in the tungstate $Tl_2W_4O_{13}$ (Goreaud, Labbé, Monier & Raveau, 1979) or in tetragonal bronzes M_xWO_3, first described by Magnéli (1949), where they are delimited by WO_6 octahedra exclusively. Indeed, the minimum distance between the centre of opposite O atoms is only 3·58 (5) Å. Two adjacent tunnels are interconnected through pseudohexagonal windows delimited by the edges or faces of four octahedra and three tetrahedra as shown in Fig. 4. They have a greater 'diameter' than that of pentagonal rings: the minimum distance between opposite oxygens is 4·66 (5) Å. This framework may also be considered as forming cages bounded by eighteen O atoms. Such a cage is built from four tetrahedra and eight octahedra (Fig. 5); it shares four pentagonal faces with identical cages, located at upper and lower levels *x*, which build

Table 2. *Coordination of* W *and* P *in* $P_4W_8O_{32}$

Interatomic distances are in Å and angles in degrees.

W(1)–O(1)	1·87 (4)	O(2)–W(1)–O(4)	88·5 (16)
W(1)–O(1)	1·88 (4)	O(2)–W(1)–O(5)	87·2 (17)
W(1)–O(2)	1·98 (3)	O(2)–W(1)–O(8)	172·8 (18)
W(1)–O(4)	1·95 (3)	O(4)–W(1)–O(5)	86·6 (14)
W(1)–O(5)	1·88 (3)	O(4)–W(1)–O(8)	86·6 (15)
W(1)–O(8)	1·81 (3)	O(5)–W(1)–O(8)	87·2 (16)
W(2)–O(3)	1·96 (2)		
W(2)–O(4)	1·81 (3)	O(3)–W(2)–O(4)	92·7 (15)
W(2)–O(5)	1·87 (3)	O(3)–W(2)–O(5)	91·5 (15)
W(2)–O(6)	2·03 (3)	O(3)–W(2)–O(6)	85·7 (14)
W(2)–O(7)	2·04 (4)	O(3)–W(2)–O(7)	82·9 (15)
W(2)–O(8)	1·93 (3)	O(3)–W(2)–O(8)	173·1 (16)
P–O(2)	1·51 (3)	O(4)–W(2)–O(5)	94·1 (15)
P–O(3)	1·52 (3)	O(4)–W(2)–O(6)	177·7 (13)
P–O(6)	1·49 (3)	O(4)–W(2)–O(7)	88·6 (15)
P–O(7)	1·49 (4)	O(4)–W(2)–O(8)	91·5 (15)
		O(5)–W(2)–O(6)	87·6 (13)
		O(5)–W(2)–O(7)	173·9 (15)
		O(5)–W(2)–O(8)	93·7 (15)
O(1)–W(1)–O(1)	90·2 (18)	O(6)–W(2)–O(7)	89·6 (13)
O(1)–W(1)–O(2)	90·0 (18)	O(6)–W(2)–O(8)	89·9 (14)
O(1)–W(1)–O(2)	93·4 (18)	O(7)–W(2)–O(8)	91·7 (15)
O(1)–W(1)–O(4)	91·0 (16)		
O(1)–W(1)–O(4)	177·7 (16)	O(2)–P–O(3)	107 (2)
O(1)–W(1)–O(5)	92·3 (16)	O(2)–P–O(6)	111 (2)
O(1)–W(1)–O(5)	176·4 (16)	O(2)–P–O(7)	113 (2)
O(1)–W(1)–O(8)	95·4 (17)	O(3)–P–O(6)	109·1 (19)
O(1)–W(1)–O(8)	91·4 (17)	O(3)–P–O(7)	106 (2)
		O(6)–P–O(7)	110·9 (19)

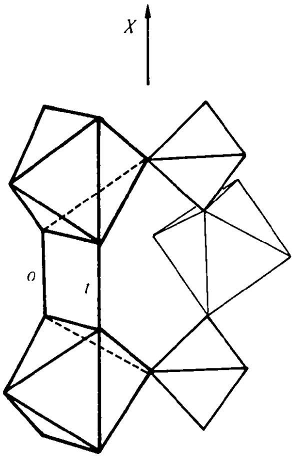

Fig. 4. Scheme of a pseudohexagonal window viewed in the **b** direction. The square face, common with an O_{12} cage, is delimited by the edges of an octahedron (*o*) and a tetrahedron (*t*) which are not drawn.

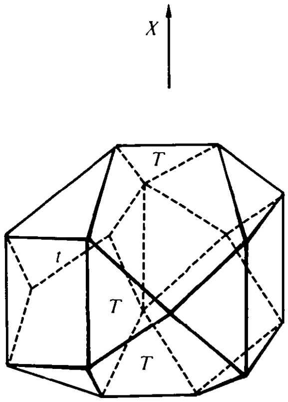

Fig. 5. Schematic representation of the O_{18} cage viewed in the **b** direction. *T* and *t* are respectively a face and an edge of a tetrahedron.

two adjacent pentagonal tunnels previously described. An O_{18} cage shares also four square faces with cages limited by twelve O atoms. These O_{12} cages are in fact perovskite cages in which a WO_6 octahedron is replaced by a PO_4 tetrahedron. The size of an O_{18} cage should allow the insertion of small cations, with a maximum radius of about 1 Å.

However, this structure exhibits an important similarity with the $Rb_xP_8W_{8n}O_{24n+16}$ structures: it is built up of ReO_3-type slabs parallel to (001) and linked together through 'planes' of PO_4 tetrahedra (Fig. 6*b*). The 'planes' of tetrahedra determine rows of pentagonal tunnels parallel to (001), in the same manner as the P_2O_7 groups form rows of distorted hexagonal tunnels parallel to the perovskite slabs in the $Rb_xP_8W_{8n}O_{24n+16}$ family. In $P_4W_8O_{32}$, the width of the ReO_3-type slabs is in fact determined by units of corner-sharing octahedra extending approximately along [021] and [$0\bar{2}1$]. These units consist of strings of two WO_6 octahedra ($n = 2$), limited by the tetrahedra (Fig. 1 and Fig. 6*b*). Therefore this oxide can be considered as the second member of a series of microphases $P_4W_{4n}O_{12n+8}$ for which *n* determines the width of the ReO_3-type slabs. Hypothetical structures with $n = 1$ and $n = 3$ are shown as examples in Fig. 6(*a*) and (*c*).

These results show a possibility for PO_4 tetrahedra to accommodate an ReO_3-type framework.

All the cavities of the structure being empty, this structural type can thus be considered as an 'opened framework' in which cations with a suitable size, such as Li^+, Na^+ or Ca^{2+}, could be intercalated and should be able to exhibit a certain mobility owing to the interconnection of the cavities. The electrical properties of the phases $P_4W_{4n}O_{12n+8}$ and of related compounds will be investigated.

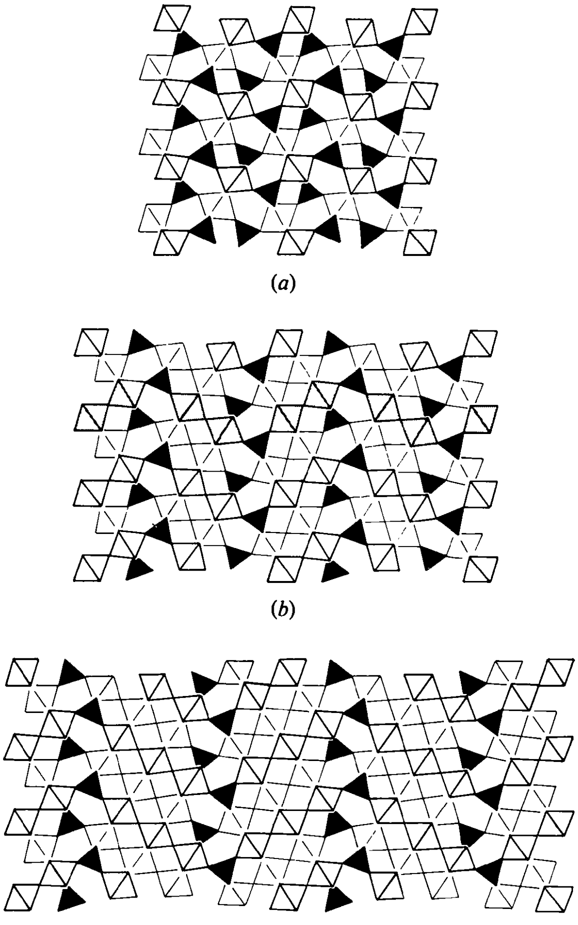

Fig. 6. The first members of the series $P_4W_{4n}O_{12n+8}$. (*a*) Hypothetical structure for $n = 1$. (*b*) $n = 2$: stippled octahedra belong to the same chain. (*c*) Hypothetical structure for $n = 3$.

References

Cromer, D. T. (1965). *Acta Cryst.* **18**, 17–23.

Cromer, D. T. & Waber, J. T. (1965). *Acta Cryst.* **18**, 104–109.

Giroult, J. P., Goreaud, M., Labbé, Ph. & Raveau, B. (1980). *Acta Cryst.* B**36**, 2570–2575.

Giroult, J. P., Goreaud, M., Labbé, Ph. & Raveau, B. (1981). *Acta Cryst.* B**37**, 1163–1166.

Goreaud, M., Labbé, Ph., Monier, J. C. & Raveau, B. (1979). *J. Solid State Chem.* **30**, 311–319.

Kierkegaard, P. (1958). *Acta Chem. Scand.* **12**, 1715–1729.

Labbé, Ph., Goreaud, M., Raveau, B. & Monier, J. C. (1979). *Acta Cryst.* B**35**, 1557–1564.

Magnéli, A. (1949). *Ark Kemi*, **1**, 213–221, 269–272.

Magnéli, A. (1956). *J. Inorg. Nucl. Chem.* **2**, 330–339.

Schulz, I. (1955). *Z. Anorg. Allg. Chem.* **281**, 99–112.

Suzuki, T. (1960). *Acta Cryst.* **13**, 279.